DOI: 10.1002/ejic.200600635

Solvent-Induced Pore-Size Adjustment in the Metal-Organic Framework $[Mg_3(ndc)_3(dmf)_4]$ (ndc = naphthalenedicarboxylate)

Irena Senkovska[a] and Stefan Kaskel*[a]

Keywords: Metal-organic frameworks / Magnesium / Carboxylate ligands / Adsorption

Two new compounds containing magnesium and the bidentate ligand 2,6-naphthalenedicarboxylate (ndc), namely $[Mg(dmf)_2(H_2O)_4]$·ndc (**1**) (dmf = *N*,*N*-dimethylformamide) and $[Mg_3(ndc)_3(dmf)_4]$ (TUDMOF-2) (**2**), have been obtained from $Mg(NO_3)_2$·$6H_2O$ and the pure acid using a solvothermal route. According to single-crystal X-ray studies both compounds are monoclinic. Complex **1** crystallizes in the space group $P2_1/c$ [a = 12.317(3), b = 12.582(2), c = 15.353(3) Å, β = 110.96(3)°]. The compound consists of an isolated tetraaquabis-*N*,*N*-dimethylformamide cation and the deprotonated ligand with hydrogen bonds linking the cations and anions. The metal-organic framework **2** crystallizes in the space group $C2/c$ [a = 13.451(3), b = 18.043(4), c = 20.937(5) Å, β = 99.79(3)°] with trinuclear magnesium clusters connected to six dicarboxylate ligands that link the clusters into a three-dimensional network. In contrast to $[Mg_3(ndc)_3(def)_4]$ (def = *N*,*N*-diethylformamide; **3**), the dmf molecules coordinated to magnesium in TUDMOF-2 (**2**) not only cause a distortion of the network but induce accessibility for the adsorption of nitrogen. TUDMOF-2 has a Langmuir surface area of 520 $m^2 g^{-1}$ and a hydrogen adsorption capacity of 0.78 wt.-% at 77 K and 760 Torr.

Introduction

Metal-organic frameworks (MOFs) are a new family of porous crystalline inorganic–organic hybrid materials that are attracting increasing interest due to their rich structural chemistry and potential applications in gas storage, separation processes, and catalysis.[1] The modular concept allows for a rational design of porous solids in which a multinuclear complex (cluster) is used as a connecting node and an organic bi- or trifunctional linker to link the nodes into a three-dimensional network of predefined topology. An often observed structural motif in transition metal MOFs is the paddle-wheel unit acting as a four-connecting node.[2] Such copper-, zinc-, or molybdenum-containing networks may be useful for hydrogen storage applications.[3] The most prominent 6-connector is the Zn_4O^{6+} cluster in MOF-5 and the IRMOF family.[4]

Although transition-metal-containing MOFs have been widely investigated, the coordination chemistry of alkaline earth metals has until now remained a largely underdeveloped area, and reports on magnesium coordination polymers are very rare.[5] Magnesium carboxylates seldom form coordination polymers and extended three-dimensional structures because of the high affinity of Mg^{2+} for oxygen donor atoms of polar solvents. Additionally, the coordination chemistry of magnesium is less flexible than that of zinc, and octahedral complexes are often found.[6] In the case of polyfunctional ligands used for the synthesis of Mg-based MOFs, competitive coordination by water or other solvent ligands may result in low-dimensional network topologies or isolated complexes, and thus porosity cannot be expected. However, the first magnesium-based metal-organic framework with permanent porosity and accessibility for very small molecules (H_2, O_2) was recently reported by Dinća and Long.[7] $[Mg_3(ndc)_3(def)_4]$ (**3**) (def = *N*,*N*-diethylformamide) was found to adsorb O_2 and H_2 preferentially, although the pores were too small to allow the access of N_2.

Below we describe the structure of two new magnesium carboxylates, namely $[Mg(dmf)_2(H_2O)_2]$·ndc (**1**) and $[Mg_3(ndc)_3(dmf)_4]$ (TUDMOF-2, **2**). TUDMOF-2 (Technical University Dresden Metal Organic Framework no. 2) has the same network topology as $[Mg_3(ndc)_3(def)_4]$ but the smaller solvent molecule induces significant structural changes, resulting in a larger pore diameter and permanent porosity with pores accessible for N_2 molecules.

Results and Discussion

Synthesis and Structural Characterization of 1 and 2

Solvothermal reaction of $Mg(NO_3)_2$·$6H_2O$ and ndc in dmf at 110 °C results in the formation of yellow crystals of **2**. White crystals of **1** were obtained from the same reaction carried out in aqueous dmf (5 vol-% H_2O). In spite of their

[a] Department of Inorganic Chemistry, Technical University Dresden
Mommsenstr. 6, 01069 Dresden, Germany
Fax: +49-351-4633-7287
E-mail: Stefan.Kaskel@chemie.tu-dresden.de

very similar synthetic conditions, complexes **1** and **2** have completely different architectures.

Single-crystal X-ray diffraction was used to determine the structure of compound **1**. Instead of carboxylate ligands coordinating to Mg^{2+}, the compound consists of isolated $[Mg(H_2O)_4(dmf)_2]^{2+}$ cations and ndc^{2-} anions (Figure 1). The Mg^{2+} ion has a sixfold coordination and is surrounded by four water molecules and two oxygen atoms of dmf molecules, resulting in a somewhat distorted octahedral geometry. Figure 2 shows a packing diagram of **1**. Hydrogen bonds link the water molecules to the carboxylate O atoms (O···O = 2.68–2.75 Å) to form a three-dimensional hydrogen-bonded network.

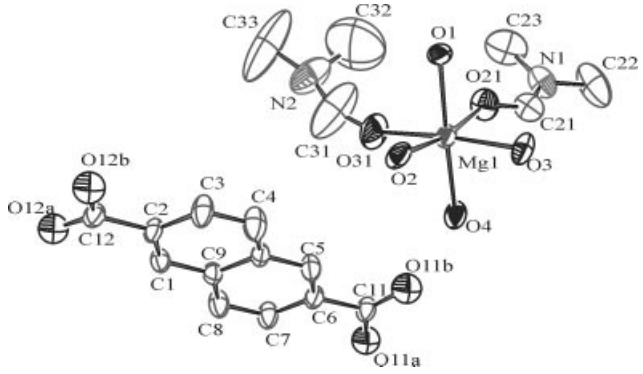

Figure 1. The asymmetric unit and labelling scheme for compound **1**. Displacement ellipsoids are drawn at the 50% probability level. H atoms have been omitted.

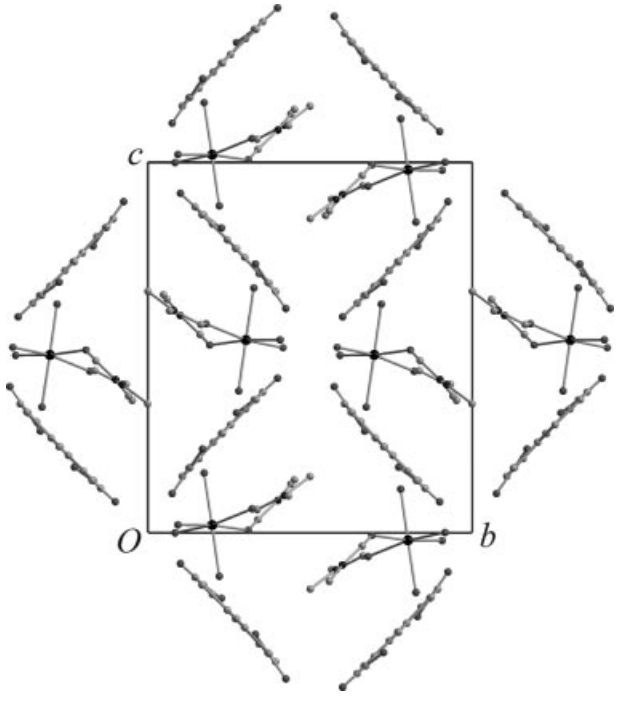

Figure 2. The crystal packing of **1** viewed along the crystallographic *a* axis.

Complex **2** crystallizes in the monoclinic space group *C*2/*c* and is a structural analogue of $[Mg_3(ndc)_3(def)_4]$ (**3**) reported by Dinća and Long.[7] However, the channels in **2** are filled with dmf instead of def, which results in a significantly reduced lattice constant *a* of 13.451 Å compared to that of **3** (*a* = 15.045 Å). All other lattice parameters are very close to those reported for **3** with differences of below 0.1 Å for *b* and *c* and below 2° for the monoclinic angle.

The structure of **2** contains two independent magnesium centers (Figure 3a). Mg1 is positioned on a twofold rotation axis and Mg2 is located at a general position (*8f*). The ndc^{2-} anions are positioned on an inversion center located in the middle of the central C–C bond in the naphthalene system. Two distinct carboxylate coordination modes are observed. The C16 and C26 carboxylate groups form didentate bridges, whereas the C6 carboxylate group chelates to Mg2, with each of the O atoms also bound to Mg1. This tridentate bridging mode is postulated to be an important intermediate in "carboxylate-shift" chemistry[8] and is a key factor for the formation of the trinuclear metal cluster. Consequently, Mg1 is connected to two adjacent Mg2 centers to form a linear $[Mg_3(\mu_3\text{-}O)_2(\mu_2\text{-}O)_4]$ unit with a nonbonding Mg–Mg distance of 3.582(6) Å (Figure 3a). These trinuclear magnesium clusters represent a 6-connecting secondary building unit (Figure 3b).[9] They are linked by naphthalenedicarboxylate bridges to form a three-dimensional network (Figure 3c and Figure 4).

A trinuclear SBU has been reported earlier as a discrete molecular cluster.[10] Furthermore, this structural motif has been found in networks such as $Zn_3(bdc)_3{\cdot}6CH_3OH$ (bdc = benzenedicarboxylate) (MOF-3),[11] $[Cd_3(bdc)_3(L)_2(H_2O)_2]$ (L = 1,4-bis(1,2,4-triazol-1-yl)butane),[12] $[CoT(p\text{-}CO_2)PPCo_{1.5}(C_5H_5N)_3(H_2O)]{\cdot}11C_5H_5N$ (PIZA-1),[13] and $[Co_3(bpdc)_3(bpy)]{\cdot}4dmf{\cdot}H_2O$ (bpdc = biphenyldicarboxylate, bpy = 4,4′-bipyridine) (IRPM-1),[14] each of which contains M^{II}_3 clusters linked together to form a rigid framework with accessible internal channels and/or cages and permanent porosity.

In contrast to the compressed central MgO_6 octahedron of Mg1 in **3**, the magnesium–oxygen octahedron in the trinuclear cluster of **2** is elongated, with axial Mg1–O61 bond lengths of 2.109(3) Å and equatorial bond lengths of 2.077(3)–2.084(3) Å. The three Mg^{2+} ions in the trinuclear motif form an almost linear chain. The Mg2–Mg1–Mg2^i (symmetry code: *i*: –*x*, *y*, 1/2 – *z*) angle in the Mg_3 units of **2** is 174.36(7)° and is thus somewhat smaller than the corresponding angle in **3** [176.14(1)°].

The Mg1–Mg2 distance in **2**, however, is longer than in **3** [3.530(2) Å] because of the longer Mg–O bonds in the former. Thus, the structural changes within the Mg_3 cluster are not responsible for the compressed *a* axis, whereas the orientation of the linker in the 6-connecting SBU allows for compression or elongation along the *a* axis, resulting in a high flexibility and breathing of the $Mg_3(ndc)_3$ network.

The reason for the contraction along the *a* axis observed in **2** as compared to **3** is the predefined orientation of solvent molecules upon coordination to Mg2. The ethyl groups of the def molecules in **3** are oriented along the *a* axis and thus occupy more space in this direction. The orientation is similar for dmf in **2**, thus allowing for a compression along the *a* axis. The dmf molecules in **2** can be re-

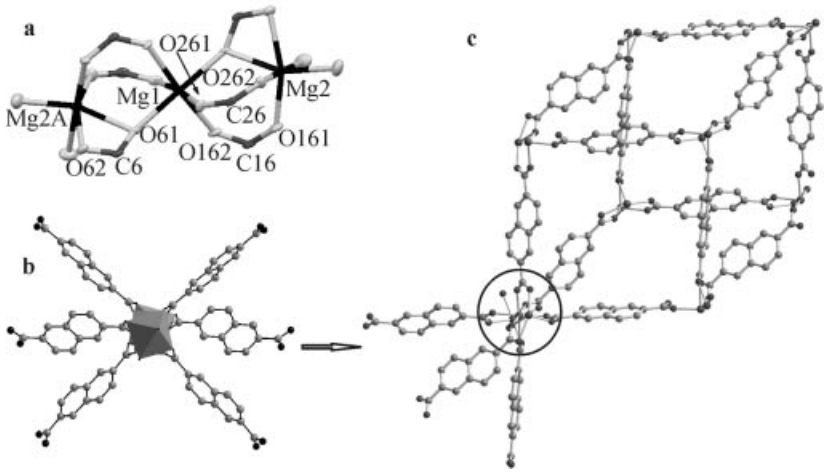

Figure 3. a) Trinuclear Mg-carboxylate cluster; b) representation of the inorganic 6-connecting SBU; c) the three-dimensional network in **2**.

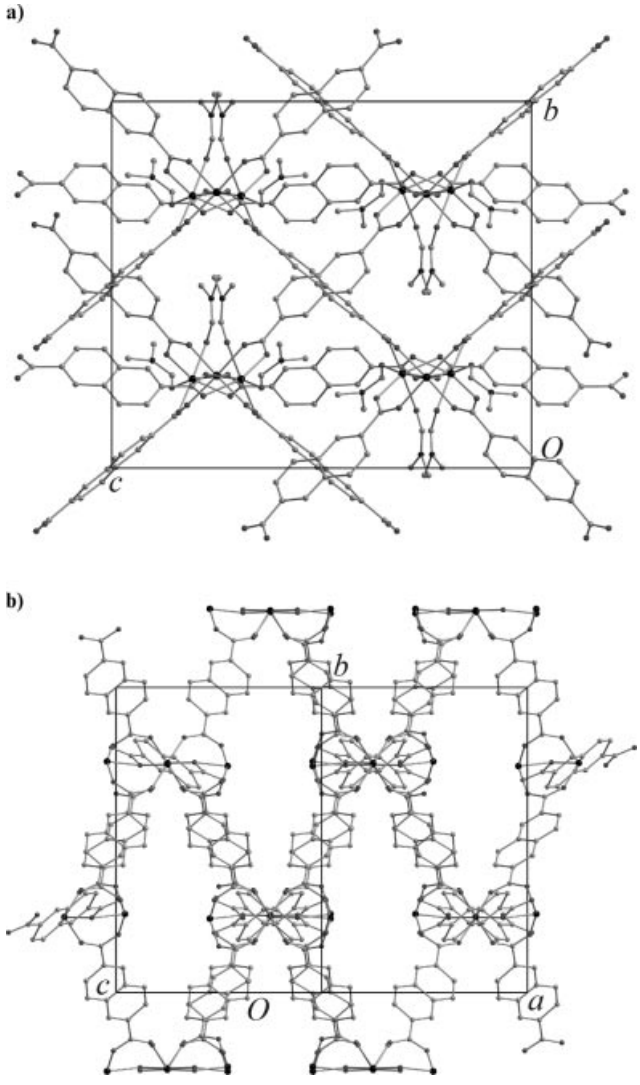

Figure 4. Extended structure of **2** viewed along: a) the crystallographic *a* axis; b) along [101] (dmf molecules have been omitted).

moved from the voids to give a porous network having open magnesium sites. This open framework has channels along the [100] and [101] directions (Figure 4). The minor differences in structure cause significant changes in the gas adsorption properties of **2** and **3**.

Thermal Stability

Thermogravimetric analysis (TGA) shows the desolvation of compound **1** in one step at a temperature above 90 °C. The weight loss of 41% for **1** from 90 to 170 °C corresponds to the loss of four H_2O and two dmf molecules from the structure (calcd.: 42.13%). The second step in the range from 500 to 540 °C indicates the decomposition of the ligand.

The framework of **2** has a high thermal stability up to 500 °C. For compound **2**, a total weight loss of 29% is observed between 120 and 400 °C, corresponding to four dmf molecules per Mg_3 unit. This weight loss is consistent with the elemental analysis and the empirical formula deduced from the single-crystal X-ray analysis. The desolvated framework is hereafter denoted as **2a**. The X-ray powder diffraction pattern of **2** changes after removal of the guest molecules as compared to the product obtained from the solvothermal synthesis. The reflections of **2a** show an apparent shift to the lower angle region, and several of the reflections disappear (Figure 5b), thereby indicating a slight structural deformation of the framework upon desolvation. After treatment of **2a** with dmf, the virgin framework of **2** regenerates (Figure 5a), thus indicating a reversible transformation (Scheme 1).

However, some additional peaks appear too. Treating **2a** with def molecules should afford **3** (Figure 5c) and, due to the larger size of the def molecules, the latter is expected to expand the lattice constant *a* as discussed above. This host flexibility can improve the efficiency of the adsorption by the aid of host structural transformation suited for the guest molecules.[15] The XRD pattern of **2a** shows diffraction peaks similar to those of desolvated **3**. The evacuated framework of **3** is hereafter indicated as **3a**. However, a detailed comparison of the XRD patterns reveals a significant

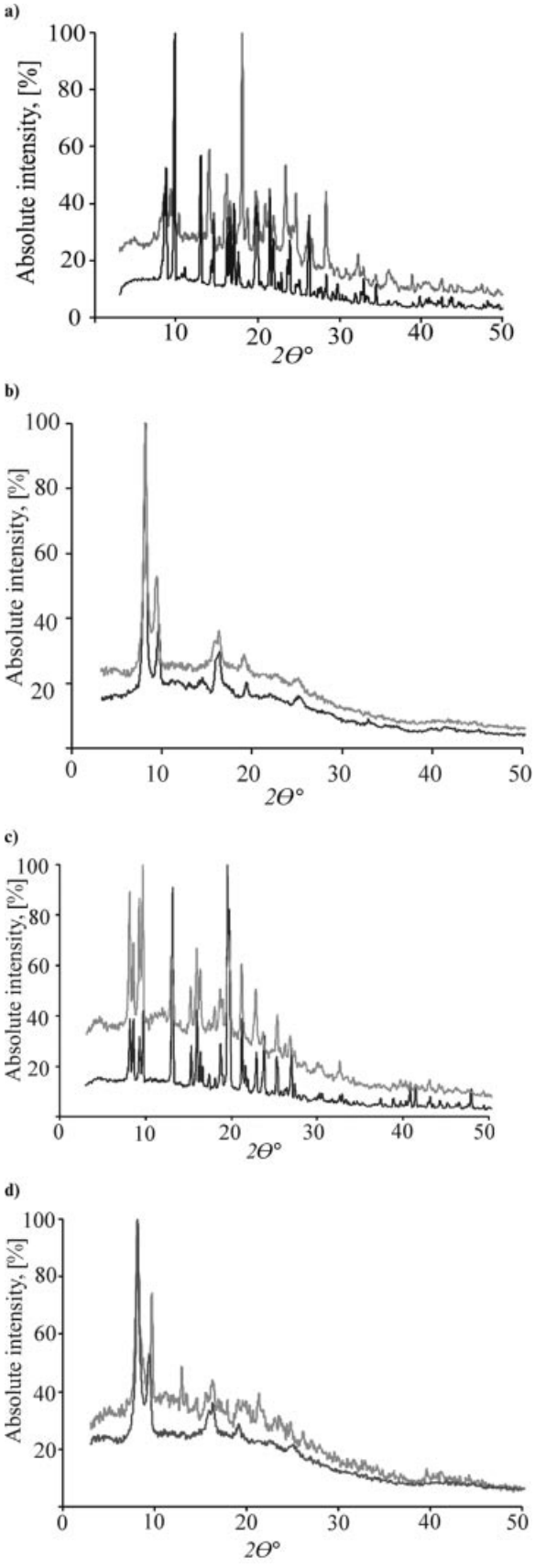

Figure 5. X-ray powder diffraction patterns: a) for **2** as synthesized (black) and **2a** resolvated with dmf (grey); b) for **2a** (black) and **3a** (grey); c) for **3** as synthesized (black) and **2a** resolvated with def (grey); d) for **3a** (black) and **3a** resolvated with dmf (grey).

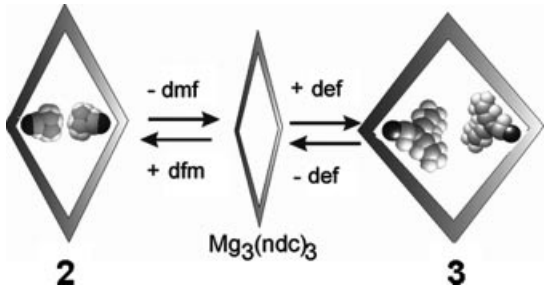

Scheme 1. The reversible structural transformation of **2** and **2a**.

shift for selected peaks (Figure 5b). Treating **2a** with def affords an XRD pattern identical to that of the as-synthesized **3** (Figure 5c). On the other hand, treating **3a** with dmf does not allow us to convert the framework into compound **2** (Figure 5d). Thus, **2** can be converted into **3** via **2a** but not vice versa. The porous materials **2a** and **3a** obtained from the different networks show small structural differences according to the X-ray powder patterns. This resembles a sort of memory effect induced by the different solvents and causes different sorption properties for the two compounds.

Sorption Properties

Compound **1** is essentially nonporous and has only a low N_2 adsorption capacity and a type II adsorption isotherm (Figure 6). Compound **2** shows a type I nitrogen adsorption isotherm at 77 K typical of a microporous material (Figure 6). The sorption isotherm was fitted to a Langmuir equation, resulting in a specific surface area of 520 $m^2 g^{-1}$ for the activated framework.

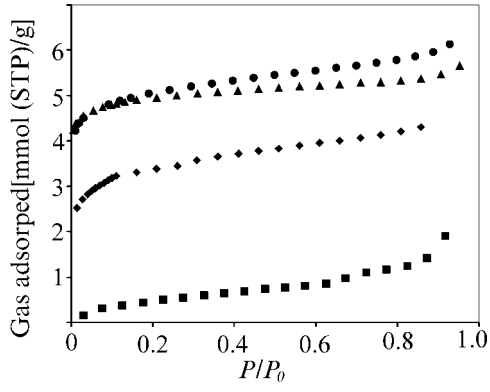

Figure 6. The N_2 (triangle), O_2 (circle), and CH_4 (diamond) adsorption isotherms of $[Mg_3(ndc)_3]$ (**2a**) and the N_2 (square) adsorption isotherm of $[Mg(dmf)_2(H_2O)_2]$·ndc (**1**) at 77 K.

Significant differences between $[Mg_3(ndc)_3(dmf)_4]$ (**2**) and $[Mg_3(ndc)_3(def)_4]$ (**3**) are also observed in the gas adsorption properties. The as-synthesized sample of **2** was activated by drying under vacuum at 468 K for 72 h. The mass loss of 28.8% was close to the 29.0% estimated for complete removal of four dmf molecules.

Whereas for **3** essentially no N_2 adsorption was detected, for TUDMOF-2 (**2**) the adsorbed amount of nitrogen (5.0 mmol g^{-1} at 0.9 P/P_0) is surprisingly large. TUDMOF-2 also shows a type I isotherm for the adsorption of CH_4 (kinetic diameter of 3.8 Å) (Figure 6). However, only oxygen and hydrogen adsorption was observed for **3**, thus indicating a limited accessibility only for smaller gas molecules due to the small pore size. The limited accessibility of nitrogen in **3** could indicate incomplete removal of def molecules in the activation, which would cause pore blocking for larger molecules such as N_2. The latter is reasonable due to the higher boiling point and more effective encapsulation of def as a result of the larger size of def relative to dmf. Thus, even though a compression of the *a* axis is detected for **2**, the more effective removal of dmf is responsible for a larger pore size in the desolvated form and larger specific pore volume. Another reason for the differences in porosity are the structural differences of **3** and **2**, which result in a memory effect and cause structural differences also in the desolvated forms of **3** and **2**. An indication for the latter is the experimentally observed difference in the XRD powder patterns of the activated forms.

The hydrogen adsorption isotherms measured at 77 K are shown in Figure 7. The hydrogen storage capacity is 3.9 mmol g^{-1} (0.78 wt.-%) at 760 Torr and is thus slightly higher than for $[Mg_3(ndc)_3(def)_4]$ but lower than for other MOFs.[3]

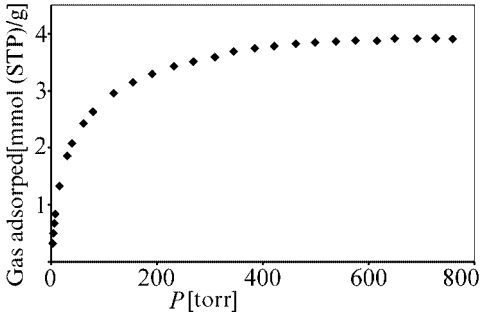

Figure 7. H_2 adsorption isotherm of $[Mg_3(ndc)_3]$ (**2a**) at 77 K.

In summary, we have presented two new magnesium carboxylates. Whereas in the presence of water molecules preferred coordination of H_2O and dmf hinders the formation of extended three-dimensional networks, a porous network structure is obtained in the absence of water. The resulting $[Mg_3(ndc)_3(dmf)_4]$ network is microporous, and the pores are accessible for H_2, O_2, N_2, and CH_4. Small structural changes induced by coordinating dmf molecules play a key role in adjusting the pore size of the network and are responsible for the size exclusion of nitrogen.

Due to the low weight of magnesium, the design of Mg-MOFs with higher specific surface areas is, in principle, feasible, although identification of suitable structural building units allowing for a high porosity remains a challenge.

Experimental Section

General: All chemicals (Aldrich) were reagent grade and were used as received. Microanalyses (C, H, N) were performed with a Fison's EA1108 CHNS analyzer. IR spectra were recorded as KBr discs using an Excalibur FTS 3000 spectrometer in the range 480–4000 cm^{-1}. Powder X-ray diffraction (PXRD) data were collected on a Stoe STADI P powder diffractometer with Cu-$K_{\alpha1}$ radiation. Thermogravimetric analyses were carried out using a Netzsch STA 409 thermal analyzer. Physisorption isotherms were measured at 77 K using a Quantachrome Autosorb1C apparatus. Prior to the measurement, the samples were evacuated at 468 K for 72 h. High purity gases were used (nitrogen: 99.999%, hydrogen: 99.999%, oxygen 99.999%, methane 99.995%). To prevent condensation of O_2 and CH_4 at 77 K, the oxygen adsorption isotherm was recorded below 156 Torr and the adsorption isotherm of methane was recorded below 9.4 Torr. The specific surface areas and porosity parameters were derived from the N_2 adsorption data.

$[Mg(dmf)_2(H_2O)_4]$·ndc (1): $Mg(NO_3)_2·6H_2O$ (0.9 g, 3.5 mmol) was mixed with 2,6-naphthalenedicarboxylic acid (0.7 g, 3.24 mmol) in dmf (18 mL) and deionized water (1 mL). The solution was filled in a 40-mL Teflon liner, placed in an autoclave, heated to 373 K for 24 h, and then cooled to room temperature. Colorless crystals of **1** were isolated from the solution at room temperature after several days. Yield: 1.06 g (71%). $C_{18}H_{28}MgN_2O_{10}$ (456.73): calcd. C 47.34, H 6.18, N 6.13; found C 46.87, H 6.28, N 6.33. IR: $\nu_{C=O}$ = 1676 (s), 1659 (vs), 1606 (s), 1560 (s), 1495 (m), 1394 (s), 1358 (s) cm^{-1}.

$[Mg_3(ndc)_3(dmf)_4]$ (2): A mixture of $Mg(NO_3)_2·6H_2O$ (1.5 g, 5.85 mmol) and 2,6-naphthalenedicarboxylic acid (0.9 g, 4.16 mmol) in dmf (60 mL) was filled in a 250-mL Teflon liner, placed in an autoclave, heated to 383 K for 24 h, and then cooled to room temperature at a rate of 0.05 K min^{-1}. The resulting pale-yellow crystals were collected, washed with dmf, and dried under argon to give **2**. Yield: 0.9 g (64.2%). $C_{48}H_{46}Mg_3N_4O_{16}$ (1007.8): calcd. C 57.21, H 4.60, N 5.56; found C 56.77, H 4.36, N 5.81. IR: $\nu_{C=O}$ = 1680 (s), 1655 (s), 1621 (s), 1566 (s), 1497 (m), 1406 (vs), 1359 (m) cm^{-1}.

X-ray Crystallography: Single-crystal X-ray diffraction data for complexes **1** and **2** were recorded with a STOE IPDS I image plate diffractometer with Mo-K_α radiation. The structures were solved by direct methods with the help of SHELXS-97[16] and refined by full-matrix least-squares techniques using SHELXL-97.[17] Non-hydrogen atoms were refined with anisotropic temperature parameters, and the hydrogen atoms of the ligands and dmf molecules were refined as rigid groups. The hydrogen atoms of the water molecules of **1** were located from the difference Fourier maps. Further details of the structural analysis are summarized in Table 1.

Table 1. Summary of X-ray crystallographic data for compounds **1** and **2**.

Compound	**1**	**2**
Formula	$C_{18}H_{28}O_{10}MgN_2$	$C_{48}H_{46}O_{16}Mg_3N_4$
Molar mass	456.73	1007.82
Space group	$P2_1/c$	$C2/c$
a [Å]	12.317(3)	13.451(3)
b [Å]	12.582(2)	18.043(4)
c [Å]	15.353(3)	20.937(5)
β [°]	110.96(3)	99.79(3)
V [$Å^3$]	2221.9(9)	5007(2)
Z, $D_{calcd.}$ [g cm^{-3}]	4, 1.365	4, 1.334
Reflns. collected/unique	18500/3448	14280/2522
Reflns. obsd. [$I > 2\sigma(I)$]	1946	1973
GOF on F^2	1.038	1.009
$R1$, wR_2 (obsd.)	0.0779, 0.1939	0.0558, 0.1489
Max., min. peaks [e $Å^{-3}$]	1.162	0.532

CCDC-607099 (**1**) and -607100 (**2**) contain the supplementary crystallographic data for this paper. These data can be obtained free of charge from the Cambridge Crystallographic Data Centre via www.ccdc.cam.ac.uk/data_request/cif.

Acknowledgments

This work was supported by the German Ministry of Science and Education (BMBF: FK 03X0011B).

[1] For recent reviews regarding the development of MOFs see, for example: a) S. Kitagawa, R. Kitaura, S. Noro, *Angew. Chem.* **2004**, *116*, 2388; *Angew. Chem. Int. Ed.* **2004**, *43*, 2334; b) S. Kaskel, in *Handbook of Porous Solids*, Wiley-VCH, Weinheim **2002**, p. 1190; c) J. L. C. Rowsell, O. M. Yaghi, *Microporous Mesoporous Mater.* **2004**, *73*, 3; d) O. M. Yaghi, M. O'Keeffe, N. W. Ockwig, H. K. Chae, M. Eddaoudi, J. Kim, *Nature* **2003**, *423*, 705.

[2] a) S. S.-Y. Chui, S. M.-F. Lo, J. P. H. Charmant, A. G. Orpen, I. D. Williams, *Science* **1999**, *283*, 1148; b) K. Schlichte, T. Kratzke, S. Kaskel, *Microporous Mesoporous Mater.* **2004**, *73*, 81; c) H. Li, M. Eddaoudi, T. L. Groy, O. M. Yaghi, *J. Am. Chem. Soc.* **1998**, *120*, 8571; d) M. Kramer, U. Schwarz, S. Kaskel, *J. Mater. Chem.* **2006**, *16*, 2245.

[3] a) P. Krawiec, M. Kramer, M. Sabo, R. Kunschke, H. Fröde, S. Kaskel, *Adv. Eng. Mater.* **2006**, *8*, 293; b) B. Chen, N. W. Ockwig, A. R. Millward, D. S. Contreras, O. M. Yaghi, *Angew. Chem. Int. Ed.* **2005**, *44*, 4745; c) B. Panella, M. Hirscher, H. Puetter, U. Mueller, *Adv. Funct. Mater.* **2006**, *16*, 520.

[4] a) H. Li, M. Eddaoudi, M. O'Keeffe, O. M. Yaghi, *Nature* **1999**, *402*, 276; b) M. Eddaoudi, J. Kim, N. Rosi, D. Vodak, J. Wachter, M. O'Keeffe, O. M. Yaghi, *Science* **2002**, *295*, 469.

[5] J. L. C. Rowsell, O. M. Yaghi, *Angew. Chem.* **2005**, *117*, 4748; *Angew. Chem. Int. Ed.* **2005**, *44*, 4670.

[6] O. Carugo, K. Djinović, M. Rizzi, *J. Chem. Soc., Dalton Trans.* **1993**, 2127.

[7] M. Dinća, J. R. Long, *J. Am. Chem. Soc.* **2005**, *127*, 9376.

[8] R. L. Rardin, W. B. Tolman, S. J. Lippard, *New J. Chem.* **1991**, *15*, 417.

[9] M. Eddaoudi, D. B. Moler, H. Li, B. Chen, T. M. Reineke, M. O'Keeffe, O. M. Yaghi, *Acc. Chem. Res.* **2001**, *34*, 319.

[10] W. Clegg, I. R. Little, B. P. Straughan, *J. Chem. Soc., Chem. Commun.* **1985**, 73.

[11] H. Li, C. E. Davis, T. L. Groy, D. G. Kelley, O. M. Yaghi, *J. Am. Chem. Soc.* **1998**, *120*, 2186.

[12] X.-L. Wang, C. Qin, E.-B. Wang, Z.-M. Su, *Chem. Eur. J.* **2006**, *12*, 2680.

[13] M. E. Kosal, J.-H. Chou, S. R. Wilson, K. S. Suslick, *Nat. Mater.* **2002**, *1*, 118.

[14] L. Pan, H. Liu, X. Lei, X. Huang, D. H. Olson, N. J. Turro, J. Li, *Angew. Chem.* **2003**, *115*, 560; *Angew. Chem. Int. Ed.* **2003**, *42*, 542.

[15] K. Uemura, R. Matsuda, S. Kitagawa, *J. Solid State Chem.* **2005**, *178*, 2420.

[16] G. M. Sheldrick, *SHELXS-86*: *Program for Crystal Structure Determination*, University of Göttingen, Germany, **1986**.

[17] G. M. Sheldrick, *SHELXL-97*: *Program for Crystal Structure Refinement*, University of Göttingen, Germany, **1993/1997**.

Received: July 5, 2006
Published Online: September 25, 2006

